Multi-physics field analysis of an induction heating device

(TEAM Workshop Problem 36)

1. General description

This benchmark falls in the area of induction heating devices and could help to test methods and codes of multiphysics field analysis in a comparative way. In particular, the transient thermal analysis of a cylindrical billet made of magnetic steel is considered: the coupled-field problem is characterized by a twofold non linearity, i.e. the dependence of magnetic permeability on both field strength and temperature. Therefore, a strongly coupled field problem is considered.

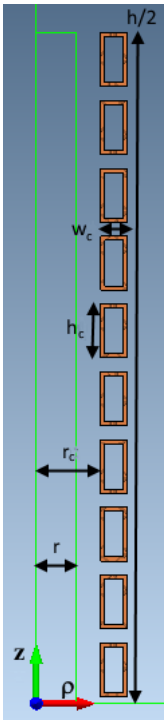

Fig. 1 - Inductor-load system geometry of the benchmark

Referring to the symbols in Fig. 1, the geometrical data of the benchmark induction heating system are those summarized in Table 1.

The electromagnetic (EM) and thermal (TH) problems can be solved using a 2D axisymmetric model. Specifically, the EM problem is solved in time-harmonic conditions, whereas the TH one is solved in transient conditions for a duration Δt=250 s, with thermal sources due to the power density induced in the billet. Due to cylindrical symmetry, the electromagnetic domain is composed of half of the inductor, half of the billet and surrounding air region; in turn, the thermal domain is composed of half of the billet. The inductor is assumed to be supplied at f = 2 kHz with a sinusoidal current with RMS value I = 3,500 A.

Table 1. Numerical data of the model geometry

Parameter	Description	Value [cm]
h	Billet axial length	100
h_{coil}=h	Inductor coil axial length	100
r	Billet external radius	3
r_c	Inductor coil internal radius	4.8
h_c	Coil turn axial length	4
w_c	Coil turn radial width	2
t_c	Copper turn conductor thickness	3

2. Material properties

The billet is made of magnetic steel with the properties listed in Tables 2-5.

Table 2. Steel electrical resistivity ρ_{el}.

°C	ρ_{el} [Ω·m]	°C	ρ_{el} [Ω·m]
0	$1.77\ 10^{-7}$	800	$1.11\ 10^{-6}$
100	$2.38\ 10^{-7}$	900	$1.16\ 10^{-6}$
200	$3.12\ 10^{-7}$	1000	$1.19\ 10^{-6}$
300	$4.00\ 10^{-7}$	1100	$1.22\ 10^{-6}$
400	$5.10\ 10^{-7}$	1200	$1.24\ 10^{-6}$
500	$6.35\ 10^{-7}$	1400	$1.25\ 10^{-6}$
600	$7.55\ 10^{-7}$	1470	$1.30\ 10^{-6}$
700	$9.50\ 10^{-6}$	1500	$1.30\ 10^{-6}$

Table 3. Steel relative permeability μ_{20} at T=20°C.

H [Am^{-1}]	0	500	1,000	1,500	2,000	2,500	3,000
μ_{20}	0	350	500	600	525	450	390
H [Am^{-1}]	4,000	8,000	15,900	23,900	39,900	79,700	159,400
μ_{20}	305	164	89.2	62.3	39.7	21	11.1
H [Am^{-1}]	239,100	318,800	358,700	398,500	477,000	557,000	
μ_{20}	7.80	6.10	5.50	5.10	4.40	3.90	

The relative magnetic permeability μ_r on temperature T and field strength H is modelled as follows:

$$\mu_r(T,H) = 1 + f(T)\cdot\mu_{20}(H) \tag{1}$$

where μ_{20} is the field-dependent relative permeability at room temperature T=20 °C (Table 3), while the function f(T) is calculated with the following relationships:

$$\begin{cases} f(T) = 1 - e^{\left(\frac{T-T_c}{C}\right)}, \; T < T_1, \; T_1 = T_c + C\ln 0.9 \\ f(T) = e^{\left(\frac{10(T_2-T)}{C}\right)}, \; T > T_1, \; T_2 = T_1 + 0.1C\ln 0.1 \end{cases} \tag{2}$$

with T_c = 770 °C the Curie temperature. Moreover, the value of constant C is usually selected by users for fitting the approximated curve with experimental data. In the benchmark the value C=20 °C is chosen.

Table 4. Thermal conductivity λ of steel

T [°C]	λ [Wm^{-1}°C^{-1}]	T [°C]	λ [Wm^{-1}°C^{-1}]
0	48.1	800	26.7
100	48.1	900	25.9
200	46.5	1000	26.7
300	44.0	1100	28.0
400	41.0	1200	29.8

500	38.5	1400	35
600	36.0	1470	39
700	31.4	1800	39
750	28.5		

Table 5. Heat capacity c_p of steel

T [°C]	c_p [Jkg^{-1}°C^{-1}]	T [°C]	c_p [Jkg^{-1}°C^{-1}]	T [°C]	c_p [Jkg^{-1}°C^{-1}]
0	481.06	1334	711.72	1422	3403.6
50	486.09	1336	712.30	1424	3473.4
100	494.04	1338	713.07	1426	3527.0
200	522.93	1340	714.07	1428	3563.3
300	561.03	1342	715.37	1430	3581.6
400	599.13	1344	717.05	1432	3581.6
500	669.89	1346	719.21	1434	3563.4
600	720.13	1348	721.98	1436	3527.1
650	749.86	1350	725.49	1438	3473.6
700	808.89	1352	729.92	1440	3403.8
710	870.02	1354	735.47	1442	3319.1
720	919.84	1356	742.39	1444	3220.9
730	1170.0	1358	750.94	1446	3111.0
747	1470.0	1360	761.45	1448	2991.2
760	1620.2	1362	774.26	1450	2863.7
770	1699.8	1364	789.77	1452	2730.3
775	1660.2	1366	808.42	1454	2593.1
780	1630.7	1368	830.68	1456	2454.1
785	1589.7	1370	857.04	1458	2315.0
787	1520.7	1372	888.05	1460	2177.6
790	1459.7	1374	924.25	1462	2043.5
800	1353.0	1376	966.18	1464	1913.9
850	979.40	1378	1014.4	1466	1790.1
900	766.15	1380	1069.4	1468	1672.8
1000	658.02	1382	1131.6	1470	1562.8
1100	655.97	1384	1201.5	1472	1460.6
1200	661.93	1386	1279.3	1474	1366.5
1300	709.69	1388	1365.3	1476	1280.6
1302	709.72	1390	1459.5	1478	1202.8
1304	709.75	1392	1561.7	1480	1133.0
1306	709.78	1394	1671.8	1482	1070.8
1308	709.81	1396	1789.1	1484	1015.9
1310	709.85	1398	1913.0	1486	967.70
1312	709.89	1400	2042.6	1488	925.83
1314	709.93	1402	2176.8	1490	889.69
1316	709.99	1404	2314.3	1492	858.73
1318	710.05	1406	2453.4	1494	832.42
1320	710.12	1408	2592.5	1496	810.22
1322	710.21	1410	2729.7	1498	791.63
1324	710.33	1412	2863.1	1500	776.17
1326	710.48	1414	2990.8	1600	820.00
1328	710.68	1416	3110.5	1700	890.11
1330	710.93	1418	3220.5	1800	900.16
1332	711.27	1420	3318.7		

3 Magnetic boundary conditions

The magnetic field problem is solved in time-harmonic conditions using a finite-element axisymmetric model (2D model) subject to boundary conditions:
tangential flux lines at ρ=0
normal flux lines at z=0.

4 Thermal boundary conditions

Convective and radiation boundary conditions are applied in the thermal problem to the billet surface. The convective exchange coefficient is assumed equal to 7 $Wm^{-2}°C^{-1}$ and the emissivity coefficient is equal to 0.8. In both conditions, T_{ext} the external temperature is equal to 70°C along lateral surface of the billet (ρ=r = 3 cm), while T_{ext} = 25°C is assumed at the end surface (z = h/2 = 50 cm).

5 Meshing the domains

The magnetic mesh should be structured according to the value of penetration depth δ

$$\delta(T,H)=\left[\pi f\sigma\mu_0\mu_r(T,H)\right]^{-1} \tag{3}$$

by generating a suitable number of element layers inside the billet close to its surface. Attention must be paid to the dependence of the penetration depth on nodal temperature through the magnetic permeability of the element. This asks for a dynamic mesh control and is a challenge for any meshing algorithm.

In turn, the thermal mesh of the billet should not be topologically coincident with the magnetic one in the same domain.

6 Comparison of FE solvers

In order to compare different solvers, the power induced in the workpiece during the heating transient can be calculated. Accordingly, after computing the magnetic field map, the transient temperature profiles at two points along the radius of the billet at z=0 should be computed: the two points can be located at ρ=0 (i.e. on the billet axis) and ρ =3 cm (i.e. on the surface of the billet). This kind of comparison versus time was shown in [1].
Alternatively, another comparison can be based on relative magnetic permeability, induced current density and temperature distribution along z=0 axis at different time instants, as shown in Figs. 2-4, respectively:

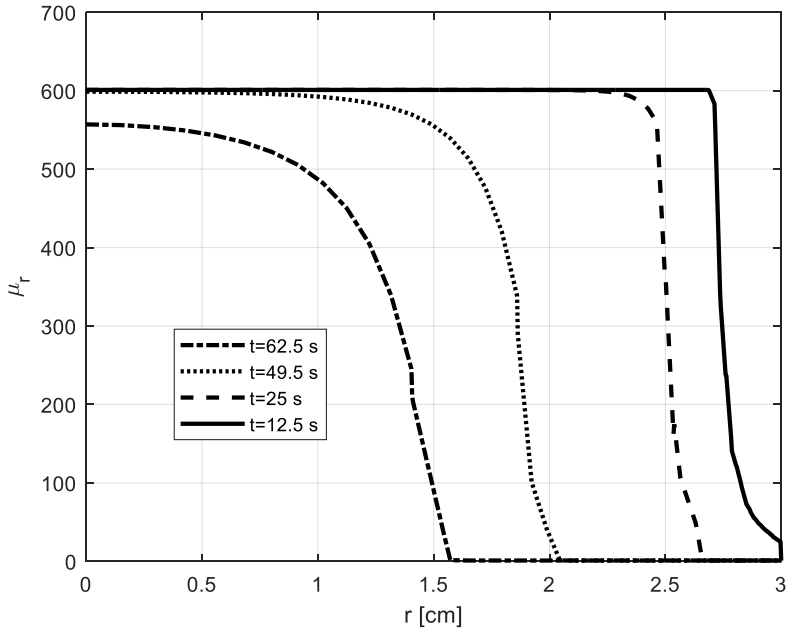

Fig. 2 - Relative magnetic permeability distribution along the billet radius at z=0, different time instants are considered.

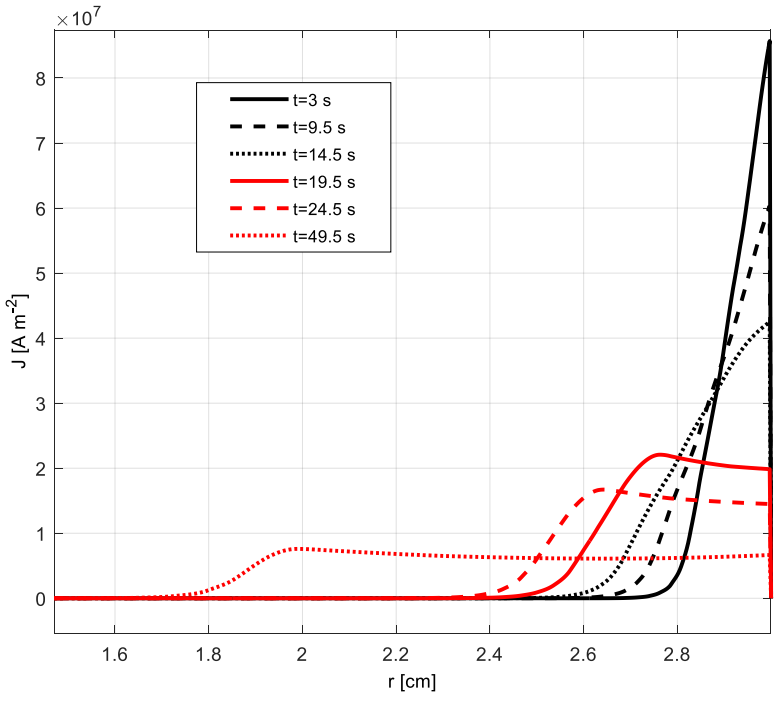

Fig. 3 – Induced current density distribution along the billet radius at z=0, different time instants are considered.

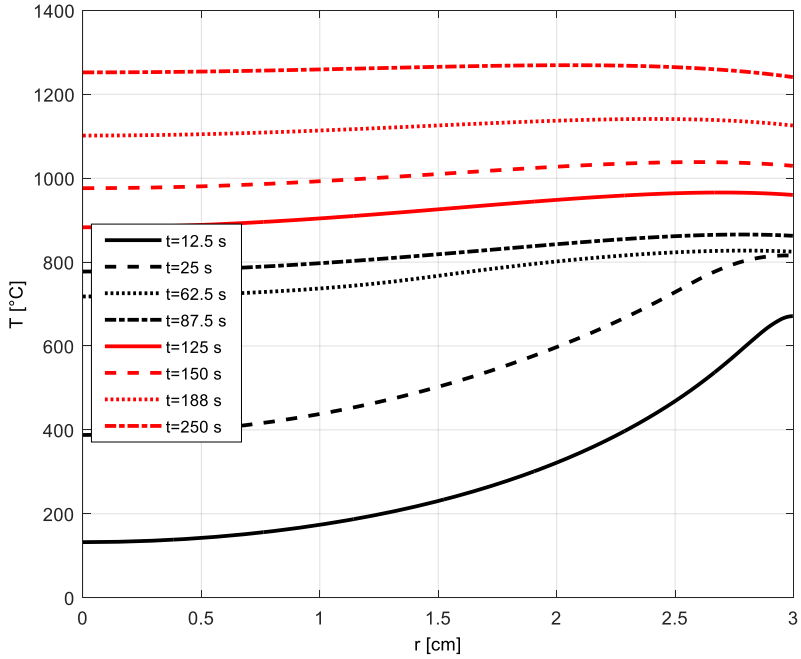

Fig. 4 - Temperature distribution along the billet radius at z=0, different time instants are considered.

References

[1] Di Barba, P., Mognaschi, M.E., Lowther, D.A., Dughiero, F., Forzan, M., Lupi, S., Sieni, E., "A benchmark problem of induction heating analysis", (2017) International Journal of Applied Electromagnetics and Mechanics, 53 (S1), pp. S139-S149.

Proposers

P. Di Barba, M.E. Mognaschi, University of Pavia
M. Forzan, University of Padova
D.A. Lowther, McGill University of Montreal